BMC Microbiology

RESEARCH Open Access

Analysis of the BadR regulon in *Borrelia burgdorferi*

Sierra George[1] and Zhiming Ouyang[1*]

Abstract

Background *Borrelia burgdorferi*, the causative agent of Lyme disease, relies on tightly coordinated gene expression to quickly adapt and survive in the tick vector and mammalian host. BadR, an ROK (repressor, open reading frame, kinase) family transcriptional regulator, binds directly to *B. burgdorferi* promoter DNA, however, many questions concerning the role for BadR in gene regulation remain unanswered. In particular, there are conflicting reports concerning what genes are regulated by BadR in *B. burgdorferi*. Furthermore, previous studies have suggested important roles for BadR in unfed ticks, but the BadR regulon has not been defined under such conditions. Additionally, although BadR regulates *rpoS* expression in a growth phase-dependent manner, it remains unknown whether BadR regulates other genes during different growth phases.

Results To address these questions, we cultivated a *B. burgdorferi badR* mutant and wild-type strain under various conditions and analyzed the transcriptome using RNA-sequencing. When spirochetes were grown at 37 °C and collected at the mid-logarithmic and stationary phase of growth, 211 and 272 genes were differentially expressed in the *badR* mutant, respectively. A total of 79 genes were differentially expressed when spirochetes were grown at 23 °C. A vast majority of genes identified in this study encode proteins of unknown function.

Conclusions Complex transcriptional regulation mechanisms coordinate the expression of genes required for the survival of *B. burgdorferi* throughout its tick-mammal enzootic lifecycle. As part of this process, BadR functions as a global regulatory protein and regulates *B. burgdorferi* virulence gene expression. Combined, this work supports a role for BadR in global *B. burgdorferi* gene regulation by modulating expression of different sets of genes at different stages of the enzootic lifecycle. We anticipate that investigating the function of genes in the BadR regulon will lead to the identification of novel virulence factors for therapeutic and vaccine development.

Keywords Lyme disease, *Borrelia burgdorferi*, Gene regulation, BadR, RNA-sequencing

*Correspondence:
Zhiming Ouyang
zouyang@usf.edu
[1]Department of Molecular Medicine, University of South Florida, 12901 Bruce B Downs Blvd, MDC 07, Tampa, FL 33612, USA

Background

Borrelia burgdorferi (aka *Borreliella burgdorferi*) survives in an enzootic lifecycle where it is transmitted between a tick vector and mammalian hosts. The cycle begins when *Ixodes scapularis* larvae acquire the bacterium from an infected small mammal during a bloodmeal. Fed larvae molt into unfed nymphs before taking a second bloodmeal and subsequently transmitting the spirochetes to a naïve host [1]. Each stage of the enzootic cycle such as tick feeding, tick molting, tick-mammal transmission, and mammalian infection poses environmental and nutritional challenges to *B. burgdorferi*, making it essential for the bacterium to quickly respond and adapt to these challenges [1–3]. For example, alterations in temperature, pH, carbon source, cell density, and osmolarity have been shown to effect *B. burgdorferi* signaling and subsequent survival in each host milieu [4–9]. Interestingly, *B. burgdorferi* lacks common or known virulence factors frequently found in other infectious bacteria and instead relies on tightly regulated gene expression to survive and cause disease. Currently, it is established that the RpoN-RpoS alternative sigma factor cascade is critical for coordinating transcription of genes required for transmission and mammalian host infection [10–13]. In this pathway, the alternative sigma factor RpoN binds to a -24/-12 promoter and transcribes *rpoS*. Once RpoS is produced, it activates a repertoire of genes essential for *B. burgdorferi* transmission and survival in the mammalian hosts, including *ospC*, *dbpA*, and *dbpB* [11, 13–16]. In addition, *B. burgdorferi* encodes several DNA and/or RNA binding proteins including BadR [17–20], BosR [21–24], Rrp2 [14, 25–27], PlzA [28–33], CsrA [34–36], and SpoVG [37, 38] which contribute to transcriptional and post-transcriptional regulation of the genome throughout the infectious cycle.

The potential role of BadR in *B. burgdorferi* pathogenesis and gene regulation was first reported by Miller et al. [17]. By analyzing the infectivity of a mutant deficient in *badR*, Miller et al. reported that the *badR* mutant was incapable of infecting mice. Moreover, expression of *rpoS* was upregulated in the *badR* mutant, suggesting that BadR represses *rpoS* expression. This critical role of BadR in *B. burgdorferi* infectivity and virulence was substantiated in a study by Ouyang et al. [18]. Specifically, Ouyang et al. found that BadR regulated expression of *rpoS* and *ospC* in a growth phase-dependent manner. However, a more recent study by Arnold et al. reported that expression of *rpoS* and RpoS-dependent genes was not changed when *badR* was inactivated [20]. These incongruous results have confounded our understanding of the role of BadR in modulating gene expression in *B. burgdorferi*. Many other important questions concerning the function of BadR in gene regulation also remain unanswered. Given that *rpoS* and the RpoS-regulon are still expressed in the *badR* mutant, the essential role of BadR in the mammalian host is possibly due to other yet-to-be-identified genes that are not regulated by RpoS. To identify those genes, the BadR regulon was previously analyzed by Miller et al. using microarray and by Arnold et al. using RNA-sequencing [17, 20]. However, a majority of putative BadR target genes identified in the study by Miller et al. were not found in the study by Arnold et al., and vice versa. Moreover, both studies only analyzed the BadR regulon in *B. burgdorferi* cultivated under conditions mimicking mammalian hosts and collected at the mid-logarithmic growth phase, but not at the late-logarithmic or stationary phases when RpoS is produced. Previous studies have also shown that *badR* is highly expressed during tick acquisition and the intermolt phases, suggesting that BadR plays an important role in such phases of infection. To date, the contribution of BadR to gene regulation under unfed tick conditions has not been investigated. To address these questions and to garner clarity on the role of BadR in *B. burgdorferi* gene regulation and Lyme disease pathogenesis, we created another mutant deficient in *badR* in *B. burgdorferi* clonal strain B31-A3. By analyzing the expression of *rpoS* and RpoS-dependent *ospC* in the *badR* mutant, our results confirmed that BadR represses *rpoS* expression in *B. burgdorferi*. We further defined the BadR regulon under various conditions using RNA-sequencing and found that different sets of genes were regulated by BadR when spirochetes were cultivated at different temperatures and/or collected at different growth phases. Under all tested conditions, BadR targets were located across the entire *B. burgdorferi* genome and were characterized into more than 20 functional categories, among which a vast majority have unknown or hypothetical functions.

Methods

Strains and culture conditions

Strains and plasmids used in this study are listed in Table S1. *B. burgdorferi* strain B31-A3 was used as the wild-type strain in this study. A *badR* knockout was generated in the B31-A3 background as we described before by using the suicide vector pOY277 [18]. *B. burgdorferi* was grown under conditions mimicking unfed ticks (i.e., 23 °C, BSK-glycerol, pH7.6) or mammalian host conditions (i.e., 37 °C, BSK-II, pH7.6). BSK-glycerol was prepared by replacing glucose with 0.6% glycerol in regular BSK-II media. Media was supplemented with streptomycin (100 μg/ml) as appropriate. Cells were collected when growth reached the mid-logarithmic phase ($\sim 5 \times 10^7$ cells/mL) or stationary phase ($\sim 1 \times 10^8$ cells/mL). Cells were pelleted by centrifugation, washed thrice with PBS, and stored at -80 °C for RNA extraction and sequencing.

Immunoblot analysis

Spirochetes were grown in BSK-II at 37 °C and collected at the mid-log and stationary phase of growth. Cell pellets were washed five times with PBS and resuspended in SDS sample buffer with 5% β-mercaptoethanol. Approximately 4×10^7 cells were loaded per lane onto a 12.5% acrylamide gel. Proteins were transferred to a nitrocellulose membrane and blocked with 2% BSA. Membranes were washed thrice with PBS-Tween. Monoclonal anti-RpoS antibody and anti-OspC monoclonal antibody were used to detect RpoS and OspC, respectively [18, 24]. To verify equal loading of samples, FlaB expression was probed with chicken IgY anti-FlaB antibody [24]. Immunoblots were developed with colormetric, 4-chloro-1-napthol substrate or chemiluminescent signal using ECL Plus Western Blotting Detection System (Thermo Fisher Scientific).

RNA isolation and qRT-PCR

RNA isolation was performed as previously described [39–42]. In brief, total RNA was isolated from *B. burgdorferi* using Trizol and purified with RNeasy Mini Kit (Qiagen). RNA was treated with TURBO DNase (Thermo Fisher Scientific) to remove residual genomic DNA and further purified using GeneJET RNA Cleanup and Concentration Kit (Thermo Fisher Scientific). Resulting RNA was converted to cDNA using SuperScript IV First-Strand Synthesis System (Thermo Fisher Scientific). qRT-PCR was performed with SYBR Green PCR Master Mix on QuantStudio Real-Time PCR system. Relative quantification of gene expression was performed using the $2^{-\Delta\Delta Ct}$ method with *B. burgdorferi flaB* as a normalization control [41, 43]. Absolute quantification of gene expression was performed by using the standard curve method as previously described [42, 44]. In brief, standard curves for *flaB*, *rpoS*, *ospC*, and *badR* were generated using 10-fold serial dilutions of pOY16, pOY17, pOY28, and pOY795, respectively. Using the standard curves, absolute copies of BadR, RpoS and OspC were quantified in wild-type strain B31-A3 and presented as copies per 100 *flaB.* Primers used in this study are listed in Table S2.

RNA-Sequencing and bioinformatic analysis

Library preparation and sequencing were performed at Azenta Life Sciences (South Plainfield, NJ, USA). In brief, RNA samples were quantified using Qubit 2.0 Fluorometer (ThermoFisher Scientific) and RNA integrity was verified in the 4200 TapeStation system (Agilent Technologies). Samples were treated with TURBO DNase (Thermo Fisher Scientific) to remove DNA and rRNA depletion was performed using QIAGEN FastSelect–5 S/16S/23S Kit (Qiagen). RNA sequencing libraries were prepared by using the NEB Next Ultra II RNA Library Preparation Kit for Illumina following the manufacturer's recommendations (New England Biolabs). Sequencing libraries were validated using the Tapestation 4200 system and quantified using Qubit 2.0 Fluorometer as well as by qPCR. Libraries were sequenced on Illumina NovaSeq instrument resulting in 45–63 million single end reads per sample. Adapter sequences and poor-quality nucleotides were removed using Trimmomatic v.0.36. Trimmed reads were mapped to the *B. burgdorferi* B31 genome (NCBI) using Bowtie2 v.2.2.6., and the FeatureCounts Subread package v.1.5.2 was used to identify unique gene hit counts. Differential gene expression analysis was performed using DESeq2 and Wald test to generate *P*-values and $\log_2$ fold changes. Only genes with *P*-value ≤ 0.05 and fold change ≥ 2 were called as differentially expressed genes.

In silico sequence and structure analysis

BadR and NagC structures were predicted using AlphaFold [45]. *E. coli* Mlc structure was obtained from the PDB database (PDB 1Z6R, Chain A). BadR, NagC, and Mlc structures were superimposed and RMSD was calculated using the align function in PyMol version 2.5.5. Clustal Omega multiple sequence alignment [46] was used to align BadR, NagC, and Mlc sequences.

Statistical analysis

Statistical significance was determined between experimental groups by unpaired Student's *t*-test, one-way analysis of variance (ANOVA) followed by Tukey test for multiple comparisons, or two-way ANOVA followed by Šidák test. All analysis, excluding RNA-sequencing analysis, was performed using GraphPad Prism version 10.1.1 (GraphPad Software).

Results

badR is expressed in *B. burgdorferi* during in vitro cultivation

In vitro culture conditions have been widely used to mimic the tick and mammal environments and study *B. burgdorferi* gene regulation by RpoN, RpoS, BosR, Rrp2, PlzA, CsrA, SpoVG, and BadR [2, 8, 10, 11, 18, 21, 25, 34, 47–49]. For example, low culture temperatures (e.g., 23 °C) and BSK supplemented with glycerol (i.e., BSK-glycerol) have been used to mimic the unfed tick conditions, whereas increased culture temperature (e.g., 37 °C) and BSK with glucose (BSK-II) have been used to mimic the environment that *B. burgdorferi* encounters in the mammalian host [8, 50–53]. Therefore, to study the role of BadR in *B. burgdorferi*, we first examined *badR* expression under various in vitro conditions via quantitative RT-PCR (qRT-PCR) using the standard curve method. As shown in Fig. 1A, in *B. burgdorferi* cultivated in BSK-glycerol at 23 °C, ~4 copies of *badR* per 100 *flaB* were

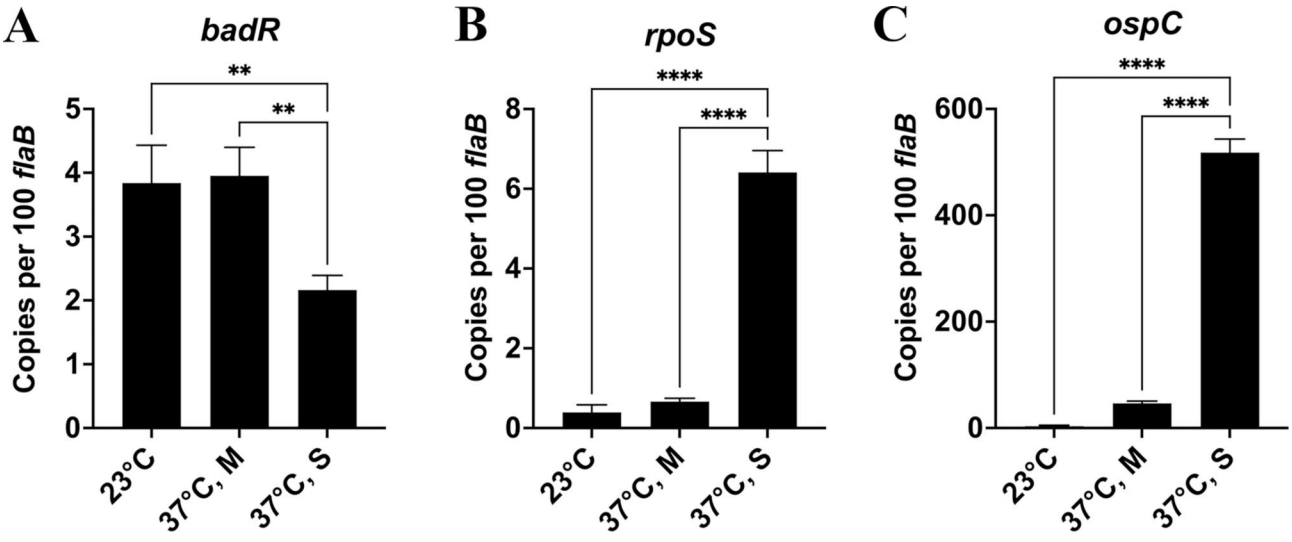

Fig. 1 Analysis of gene expression in *B. burgdorferi* grown in vitro. *B. burgdorferi* was cultivated in BSK-glycerol at 23 °C, or in BSK-II at 37 °C and collected when growth reached mid-logarithmic (M) or stationary (S) phase. Absolute quantification qRT-PCR was performed to measure transcripts of *badR* **(A)**, *rpoS* **(B)**, and *ospC* **(C)** as copies per 100 *flaB* transcripts. Data were collected from three independent replicates and the bars represent the mean values ± standard deviation. Asterisks indicate statistical significance using one-way ANOVA followed by Tukey test (**$P < 0.005$, ****$P < 0.00005$)

detected. A similar number of *badR* transcripts were detected in *B. burgdorferi* cultivated in BSK-II at 37 °C and collected at the mid-logarithmic phase ($\sim 5 \times 10^7$ cells per mL) of growth. When *B. burgdorferi* was grown in BSK-II at 37 °C and collected at the stationary phase ($\sim 1 \times 10^8$ cells per mL), ~2 copies of *badR* per 100 *flaB* were detected (Fig. 1A). As a control, expression of *rpoS* and *ospC* were also measured. Consistent with previous studies [13, 15, 18, 54], *rpoS* and *ospC* transcription was repressed in *B. burgdorferi* cultivated in BSK-glycerol at 23 °C and in BSK-II at 37 °C when collected at the mid-logarithmic phase of growth, but highly induced when spirochetes were cultivated in BSK-II at 37 °C and collected at the stationary phase (Fig. 1B, C). These results indicate that *badR* is expressed in *B. burgdorferi* under all three tested conditions during in vitro cultivation.

BadR represses expression of *rpoS* and RpoS-dependent *ospC*

Previous studies regarding BadR repression of *rpoS* have been contradictory [17, 18, 20]. Specifically, the *badR* mutants used in the studies by Miller et al. [17] and Arnold et al. [20] were derived from a clonal strain B31-A3, whereas the mutant used in the study by Ouyang et al. was generated in the nonclonal strain B31 [18]. To resolve this discrepancy, we created another *badR* mutant in the clonal strain B31-A3. qRT-PCR analysis confirmed the loss of *badR* expression in the resultant mutant (Fig. 2A). To measure the effect of BadR on *rpoS* and *ospC* expression, the wild-type (WT) strain and the *badR* mutant were grown in BSK-II at 37 °C and harvested at the mid-logarithmic and stationary phase of growth. As shown in Fig. 2B, at the mid-logarithmic phase of growth, *rpoS* transcripts were significantly increased in the *badR* mutant compared to WT. However, no significant difference in *rpoS* expression was observed at the stationary phase of growth (Fig. 2B). Similarly, *ospC* expression was significantly higher in the *badR* mutant at the mid-logarithmic phase of growth, but not at the stationary phase (Fig. 2C). RpoS and OspC protein production was further detected by immunoblot. As shown in Fig. 2D, OspC production was increased in the *badR* mutant (compared to WT) at both growth phases. Of note, in addition to the OspC band (indicated in arrows), another upper band was also detected in the mutant, but not in WT. The identity of the protein shown in the upper band remains unknown. The *badR* mutant produced higher levels of RpoS than WT at the mid-logarithmic phase of growth, but WT and the mutant produced comparable levels of RpoS at the stationary phase (Fig. 2D). As a control, similar levels of FlaB were detected in all samples (Fig. 2D). Together, these results are consistent with previous observations by Miller et al. [17]. and Ouyang et al. [18]. and substantiate that BadR regulates *rpoS* expression at 37 °C in a growth-phase dependent manner.

BadR regulates sugar transport and utilization genes in *B. burgdorferi*

Due to the limited metabolic capacity of *B. burgdorferi*, the pathogen relies heavily on the uptake of extracellular carbohydrates for survival [6, 53, 55]. At each stage of infection, different sugars are utilized by *B. burgdorferi* as the major carbohydrate source. For instance, glucose is the primary carbohydrate source in the mammalian host

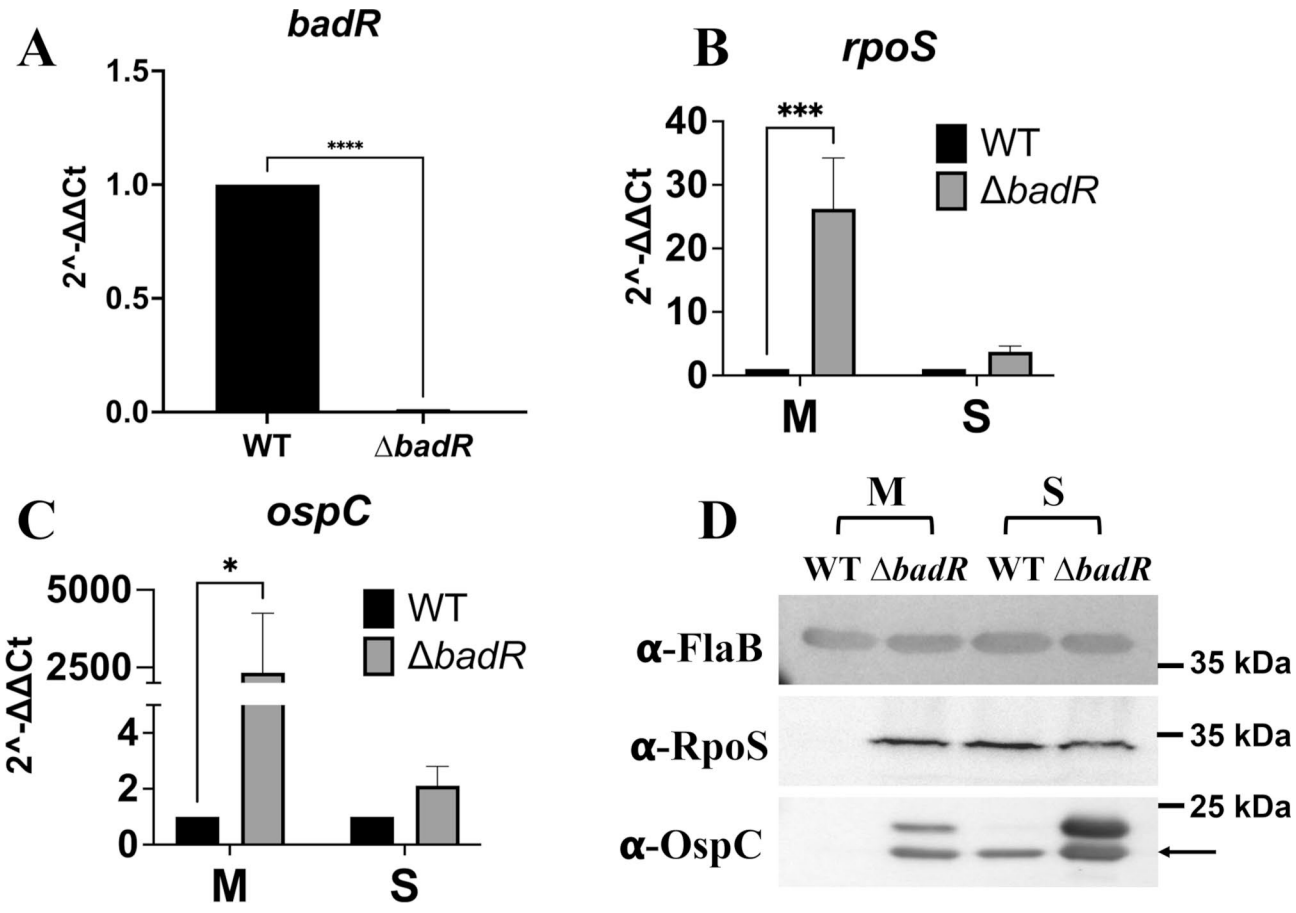

Fig. 2 BadR regulates *rpoS* expression. WT and the *badR* mutant (Δ*badR*) were grown at 37 °C in BSK-II and collected at the mid-logarithmic (M) or stationary (S) phase of growth. Relative quantification qRT-PCR was performed to measure the expression of *badR* **(A)**, *rpoS* **(B)**, and *ospC* **(C)**. Data were collected from three independent replicates and the bars represent the mean values ± standard deviation. Asterisks indicate statistical significance using one-way ANOVA followed by Tukey test or two-way ANOVA followed by Šidák test (*$P < 0.05$, *** $P < 0.0005$, **** $P < 0.00005$). **(D)** Synthesis of FlaB, RpoS, and OspC were detected in the same samples by immunoblot. A representative image of three biological replicates is shown. Specific antibodies, indicated as α-, are shown on the left and molecular weight markers are shown on the right. Arrowhead denotes OspC. Full-length immunoblots are presented in Supplementary Fig. S1-3

whereas glycerol and chitobiose (an N-acetylglucosamine dimer) are abundant in the tick microenvironment. To this end, the *B. burgdorferi* genome encodes proteins for the utilization of glucose, glycerol, chitobiose, and N-acetylglucosamine (GlcNAc) [3, 6]. Specifically, *bbb04* and *bbb05* encode chitobiose-specific phosphotransferase (PTS) components ChbA and ChbB; *bb0645*, *bbb29*, and *bb0677* encode glucose-specific PTS component PtsG, MalX2, and glucose-specific ATP-binding protein MglA; *bb0151* and *bb0152* encode GlcNAc utilization proteins NagA and NagB; and *bb0240* and *bb0241* encode glycerol kinase GlpK and glycerol-3-phosphate dehydrogenase GlpD, respectively. Given that BadR has homology to ROK (repressor, open reading frame, kinase) proteins involved in carbohydrate metabolism [56, 57], it is possible that BadR regulates genes involved in sugar transport and utilization. To test this hypothesis, we measured the expression of several carbohydrate metabolism genes in the *badR* mutant under various in vitro conditions mimicking the unfed tick (i.e., 23 °C, BSK-glycerol) and mammalian host (i.e., 37 °C, BSK-II containing glucose) by qRT-PCR (primers listed in Table S2). As aforementioned, *B. burgdorferi* grown in BSK-II at 37 °C was also collected at the mid-logarithmic or stationary phase of growth, to test the effects of growth phase on gene expression. As shown in Fig. 3A, when *B. burgdorferi* was grown at 23 °C in BSK-glycerol, expression of genes involved in glycerol utilization (*bb0240* and *bb0241*) and chitobiose transport (*bbb04* and *bbb05*) were modestly upregulated (~2-4-fold) in the *badR* mutant [50, 51]. For genes involved in glucose utilization, expression of *bbb29* was slightly upregulated (< 2-fold) and expression of *bb0645* and *bb0677* were not significantly changed. When *B. burgdorferi* was grown at 37 °C in BSK-II and collected at the mid-logarithmic phase, expression of glucose uptake/utilization genes *bb0645*

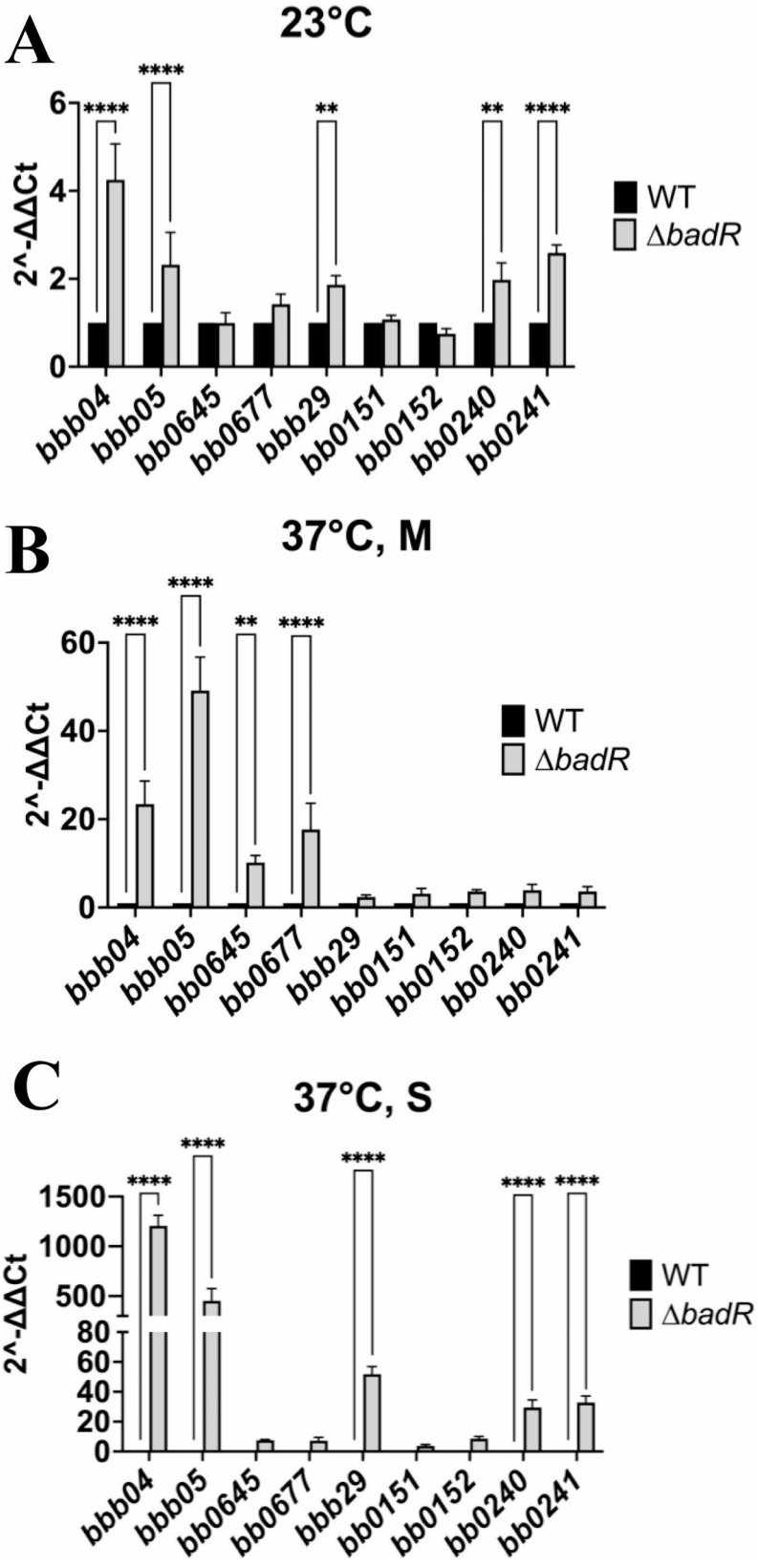

Fig. 3 (See legend on next page.)

(See figure on previous page.)

Fig. 3 BadR regulates the expression of genes involved in sugar uptake and utilization. WT and the *badR* mutant (Δ*badR*) were cultivated at 23 °C in BSK-glycerol **(A)**, at 37 °C in BSK-II to the mid-logarithmic phase **(B)**, and at 37 °C in BSK-II to the stationary phase **(C)**. Relative quantification qRT-PCR was performed to measure gene expression. M, mid-logarithmic phase; S, stationary phase. Data were collected from three independent replicates and the bars represent the mean values ± standard deviation. Asterisks indicate statistical significance using two-way ANOVA followed by Šidák test (** $P < 0.005$, **** $P < 0.00005$)

(*ptsG*) and *bb0677* (*mglA*), but not *bbb29* (*malX2*), were significantly upregulated in the mutant (Fig. 3B). Under this condition, expression of chitobiose utilization genes *bbb04* (*chbC*) and *bbb05* (*chbA*) was upregulated 23.4-fold and 49.2-fold, respectively, in the *badR* mutant, whereas expression of glycerol utilization genes was not changed (Fig. 3B). When *B. burgdorferi* was grown at 37 °C in BSK-II and collected at the stationary phase, expression of glucose utilization gene *bbb29* (*malX2*) was upregulated 51.9-fold in the *badR* mutant, but expression of *bb0645* (*ptsG*) and *bb0677* (*mglA*) remained unchanged (Fig. 3C). Furthermore, expression of glycerol utilization genes *bb0240* (*glpF*) and *bb0241* (*glpK*) and chitobiose utilization genes *bbb04* (*chbC*) and *bbb05* (*chbA*) were significantly upregulated at ~30 – 1,000-fold in the *badR* mutant (Fig. 3C). Overall, fold-change differences for these genes were significantly higher when spirochetes were cultivated at 37 °C than at 23 °C. Noteworthy is that *chbC* expression is highest during tick phases of the lifecycle compared to the mammalian host [58]. Under all tested conditions, expression of GlcNAc utilization genes *bb0151 (nagA)* and *bb0152* (*nagB*) were not significantly changed in the *badR* mutant (Fig. 3A-C). Together, these data suggest that BadR represses expression of genes involved in the uptake and utilization of chitobiose, glycerol, and glucose, and gene regulation is influenced by different growth conditions.

Genes in the BadR regulon are involved in diverse biological functions and distributed throughout the *B. burgdorferi* genome

Previous studies have suggested that BadR may function as a global transcriptional regulator in *B. burgdorferi* [17, 18, 20]. However, these studies only investigated the BadR regulon under a single in vitro condition mimicking the mammalian host (i.e., 32–34 °C, BSK-II). Moreover, these studies were performed using spirochetes collected at a single growth phase (i.e., the mid-logarithmic phase). Therefore, RNA-sequencing was performed in this study to define the BadR regulon under various conditions mimicking the unfed tick or the mammalian host. Of note, the *badR* mutant used in this study lacks two plasmids, lp28-1 and lp56. Therefore, genes located on these two plasmids were excluded from subsequent gene expression analyses. First, WT and the *badR* mutant were grown in BSK-glycerol at 23 °C (mimicking unfed ticks) and collected at the stationary phase. Under this condition, 79 genes were differentially expressed in the *badR* mutant (Fig. 4A, Table S3). When WT and the mutant were grown under condition mimicking the mammalian host (i.e., at 37 °C in BSK-II and collected at the stationary phase), RNA-sequencing revealed 272 genes differentially expressed in the *badR* mutant (Fig. 4A, Table S3). A total of 34 genes were differentially regulated by BadR under both conditions (Fig. 4B). Next, to determine whether the composition of the BadR regulon is affected by growth phases, spirochetes were grown in BSK-II at 37 °C and collected at the mid-logarithmic phase; RNA-sequencing showed that 211 genes were differentially expressed in the *badR* mutant (Fig. 4A, Table S3). Among these, 104 genes were also regulated by BadR at the stationary phase (Fig. 4B). Only 20 genes (0.04% of total genes identified) were differentially expressed in the *badR* mutant under all three tested conditions (Fig. 4B). Given that BadR represses *rpoS*, it is likely that genes we identified as regulated by BadR, may be also regulated by RpoS. Therefore, we compared the BadR regulon when grown at 37 °C to the stationary phase growth, to previously published microarray of the RpoS regulon [14, 15]. In total, 44 genes in the BadR regulon overlapped the RpoS regulon identified by Ouyang et al. [14]. and 38 genes in the BadR regulon overlapped the RpoS regulon identified by Caimano et al. [15]. These findings suggest that BadR not only influences the RpoS regulon, but also regulates other RpoS-independent genes in *B. burgdorferi*.

When *B. burgdorferi* was grown at 23 °C in BSK-glycerol, 61 genes and 18 genes, respectively, were upregulated or downregulated in the *badR* mutant (Fig. 4C and D). Moreover, 112 genes and 148 genes were upregulated, and 99 genes and 124 genes were downregulated in the *badR* mutant when *B. burgdorferi* was grown at 37 °C in BSK-II and collected at the mid-logarithmic or stationary phase, respectively (Fig. 4C and D). Across all conditions, 15 genes were upregulated including genes *bbb04*, *bbb05*, *bbb06* encoding chitobiose uptake components, *bbs41*, *bba04* encoding outer surface lipoproteins, and *bb0841* encoding an arginine deaminase [55, 59–62]. Conversely, a single gene *bbi29* encoding a virulent strain associated lipoprotein was downregulated in the *badR* mutant among all conditions. Collectively, these results suggest that BadR positively and negatively regulates *B. burgdorferi* gene expression.

Given the highly segmented nature of the *B. burgdorferi* genome and requirement for specific linear or circular plasmids during each phase of the lifecycle, differentially expressed genes were further characterized

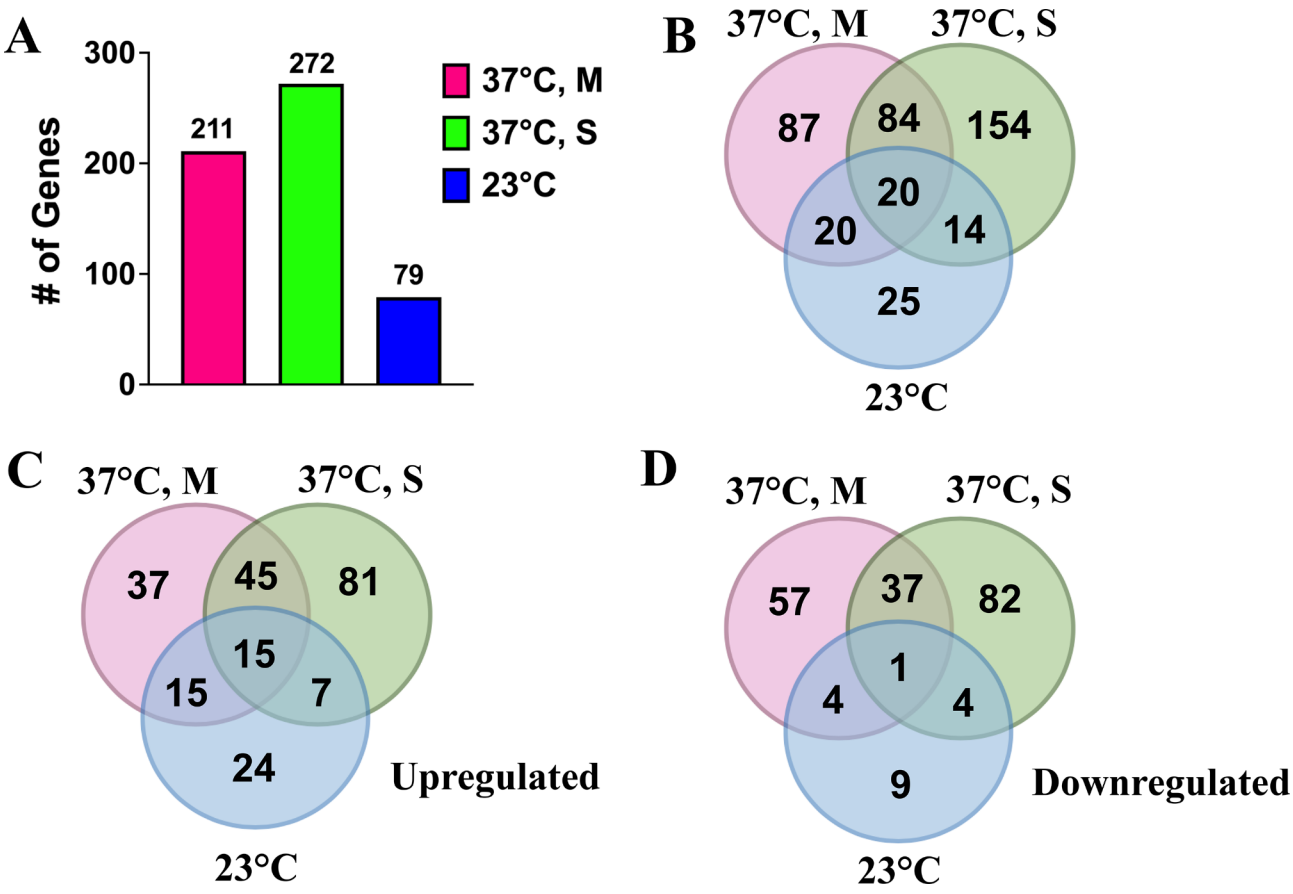

Fig. 4 Analysis of the BadR regulon. WT and the *badR* mutant were cultivated at 23 °C in BSK-glycerol, at 37 °C in BSK-II to the mid-logarithmic phase (M), and at 37 °C in BSK-II to the stationary phase (S). Gene expression was analyzed by RNA-sequencing. A gene with ≥ 2-fold change between the mutant and WT and $P \leq 0.05$ was identified as differentially regulated by BadR. **(A)** Total number of genes identified by RNA-sequencing to be differentially regulated by BadR in *B. burgdorferi* cultivated under each condition. **(B)** Venn diagram comparing total number of genes differentially expressed in the *badR* mutant. (**C**, **D**) Venn diagram comparing the number of differentially upregulated genes **(C)** and downregulated genes **(D)** in the mutant at each condition

according to genome location. As shown in Fig. 5A, when *B. burgdorferi* was grown at 23 °C in BSK-glycerol, a large number (~45%) of BadR-regulated genes were located on *lp38* and *lp54*; all of these genes were upregulated in the *badR* mutant. Notably, *lp54* encodes many differentially expressed genes required in the tick, whereas a majority of genes encoded on *lp38* have not been functionally characterized. When *B. burgdorferi* was grown at 37 °C in BSK-II and collected at the mid-logarithmic and stationary phase, ~26% and ~47% of BadR-regulated genes, respectively, were located on *cp32* family plasmids (Fig. 5B and C). Among these genes located on *cp32* plasmids, ~79% were upregulated in the mutant. Under all conditions, a large portion of genes downregulated in the *badR* mutant were located on the chromosome (Fig. 5A-C). Taken together, our data support that BadR functions as a global regulator in *B. burgdorferi*.

BadR-regulated genes were characterized into functional categories as previously annotated [55, 59, 60]. In spirochetes grown at 23 °C in BSK-glycerol, ~25% of BadR-regulated genes were annotated as encoding cell envelope associated proteins, and ~46% of genes were annotated as conserved hypothetical or having unknown function (Fig. 5D). In spirochetes grown at 37 °C in BSK-II and collected at the mid-logarithmic phase, ~38% of genes were annotated as unknown or conserved hypothetical. Other differentially expressed genes at the mid-logarithmic phase of growth were predicted to encode cell envelope associated proteins (~13%) or proteins involved in energy metabolism (~3%) and replication (~2%) (Fig. 5D). In spirochetes grown at 37 °C in BSK-II but collected at the stationary phase of growth, ~7% and ~2% of BadR-regulated genes encode cell envelope associated proteins and Bdr family proteins, respectively. Under this condition, a large portion (~30%) of genes regulated by BadR were annotated as unknown or conserved hypothetical (Fig. 5D). Interestingly, in cells (cultivated at 37 °C in BSK-II) collected at the mid-logarithmic or stationary phase of growth, ~15% and ~33%, respectively, of BadR-regulated genes were predicted to encode possible phage virion assembly proteins (Fig. 5D). In contrast, less than 5% of BadR-regulated

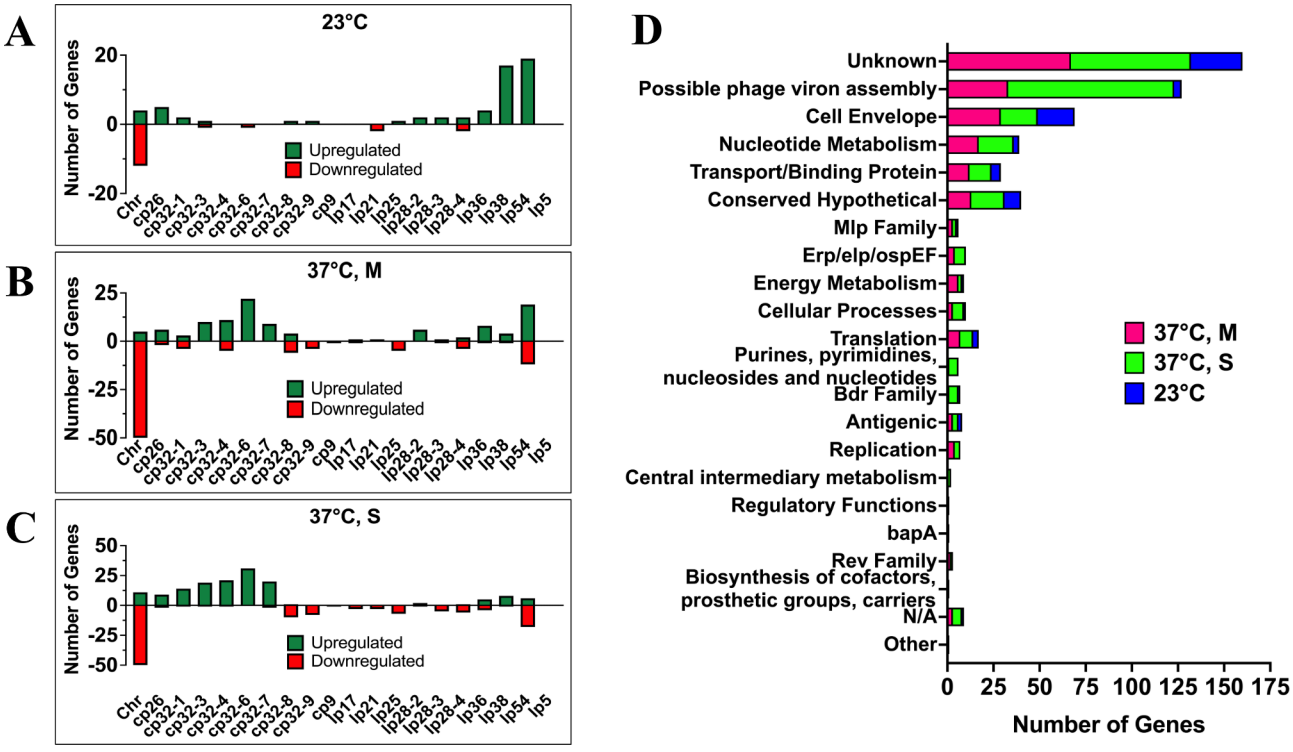

Fig. 5 Distribution and functional characterization of differentially expressed genes. (**A**-**C**) The genome location of all genes with ≥ 2-fold change and $P \leq 0.05$ between WT and the *badR* mutant when spirochetes were cultivated **(A)** at 23 °C in BSK-glycerol, **(B)** at 37 °C in BSK-II to the mid-logarithmic phase (M), and **(C)** at 37 °C in BSK-II to the stationary phase (S). **(D)** All differentially expressed genes with ≥ 2-fold change and $P \leq 0.05$ were characterized according to functional category

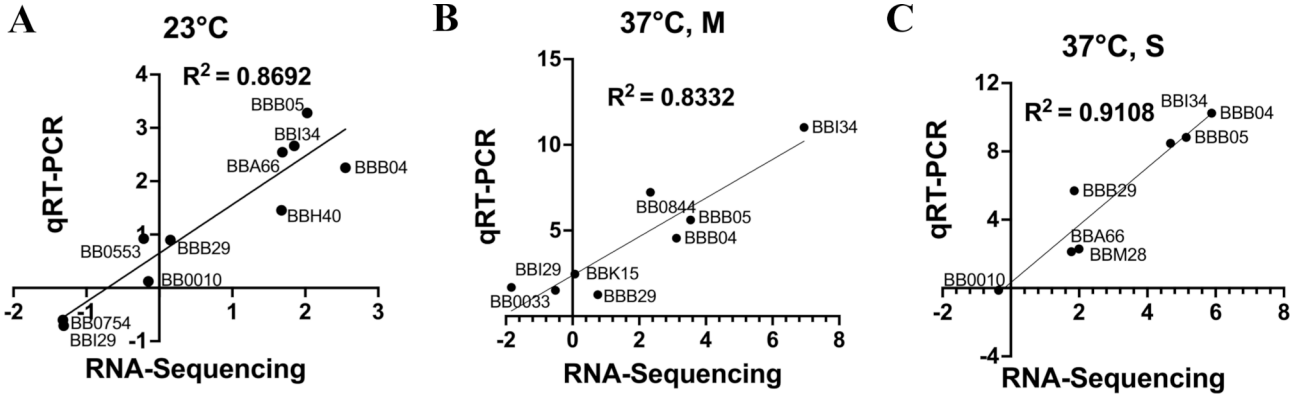

Fig. 6 Correlation between RNA-sequencing and qRT-PCR data. Log_2(fold-change) values of differentially expressed genes were plotted as black dots and labeled with gene names. Genes were selected from RNA-sequencing analyses of *B. burgdorferi* cultivated **(A)** at 23 °C in BSK-glycerol, **(B)** at 37 °C in BSK-II to the mid-logarithmic phase (M), and **(C)** at 37 °C in BSK-II to the stationary phase (S). Correlation coefficient (R^2) was calculated and labeled on each panel

genes were annotated into this category when *B. burgdorferi* was grown at 23 °C in BSK-glycerol (Fig. 5D). Across all growth conditions, differentially expressed genes were also predicted to encode Mlp family proteins, antigenic proteins, as well as proteins involved in nucleotide metabolism, transport and binding, translation, and replication (Fig. 5D).

Validation of RNA-sequencing data by qRT-PCR

To confirm RNA-sequencing results, expression of selected BadR-regulated genes was assessed between WT and the *badR* mutant by qRT-PCR (primers listed in Table S2). As shown in Fig. 6, under all three tested conditions, a strong and significant linear correlation was found when the gene expression changes determined by qRT-PCR and RNA-sequencing were compared. Specifically, linear regressions resulted in R^2 values of 0.8692,

0.8332, and 0.9108 and *P*-values of 0.0001, 0.0016, and 0.0008, when comparing RNA-sequencing and qRT-PCR gene expression analyses data of spirochetes grown in BSK-glycerol at 23 °C (Fig. 6A), in BSK-II at 37 °C and collected at the mid-log phase (Fig. 6B), or in BSK-II at 37 °C and collected at the stationary phase (Fig. 6C). These data indicate that the mRNA expression levels obtained by qRT-PCR correlated well with those obtained from RNA-sequencing analysis.

BadR has a similar structure to *E. coli* ROK proteins but lacks conserved residues for GlcNAc or glucose binding

In general, ROK proteins function as carbohydrate-responsive transcriptional repressors involved in carbon source metabolism and regulation [56, 57]. Often, binding of ROK repressors to promoter DNA is interrupted by phosphorylated sugars. For example, *E. coli* NagC regulates genes involved in the uptake and utilization of GlcNAc. NagC binds to promoter DNA and represses gene transcription in the absence of N-acetylglucosamine-6-phosphate (GlcNAc-6P). When NagC binds GlcNAc-6P via specific sugar binding residues, protein conformation is altered resulting in the dissociation of NagC from promoter DNA and subsequently gene de-repression [63]. Conversely, *E. coli* Mlc regulates genes involved in glucose uptake including PTS protein $EIICB^{Glc}$. In the absence of glucose, $EIICB^{Glc}$ is phosphorylated, and Mlc binds promoter DNA to repress transcription. In the presence of glucose, $EIICB^{Glc}$ becomes de-phosphorylated and sequesters Mlc from target DNA by direct binding, thereby promoting transcription of genes for glucose utilization [64]. Previously, BadR was predicted to be a ROK protein containing an N-terminal helix-turn-helix (HTH) DNA-binding domain and putative C-terminal sugar binding domain [17, 18]. The ability of BadR to bind target DNA via the HTH region has been confirmed [17–19]. However, the signal modulating BadR-DNA binding via the C-terminal sugar binding domain is currently unknown. To gain information regarding the function of BadR, we compared BadR with its homologues, NagC and Mlc. Sequence alignment revealed that the overall sequence homology of BadR to NagC and Mlc is only 20% and 21%, respectively (Fig. 7). In its C-terminal domain, NagC contains four residues (His194, Glu244, Gly246, and Glu266) involved in the binding of GlcNAc-6P; BadR lacks all four of these residues (Fig. 7). A single residue required for NagC and Mlc function is conserved in BadR (His247). This residue is not directly involved in sugar binding, but is essential for zinc binding and the functions of all three proteins [17, 63].

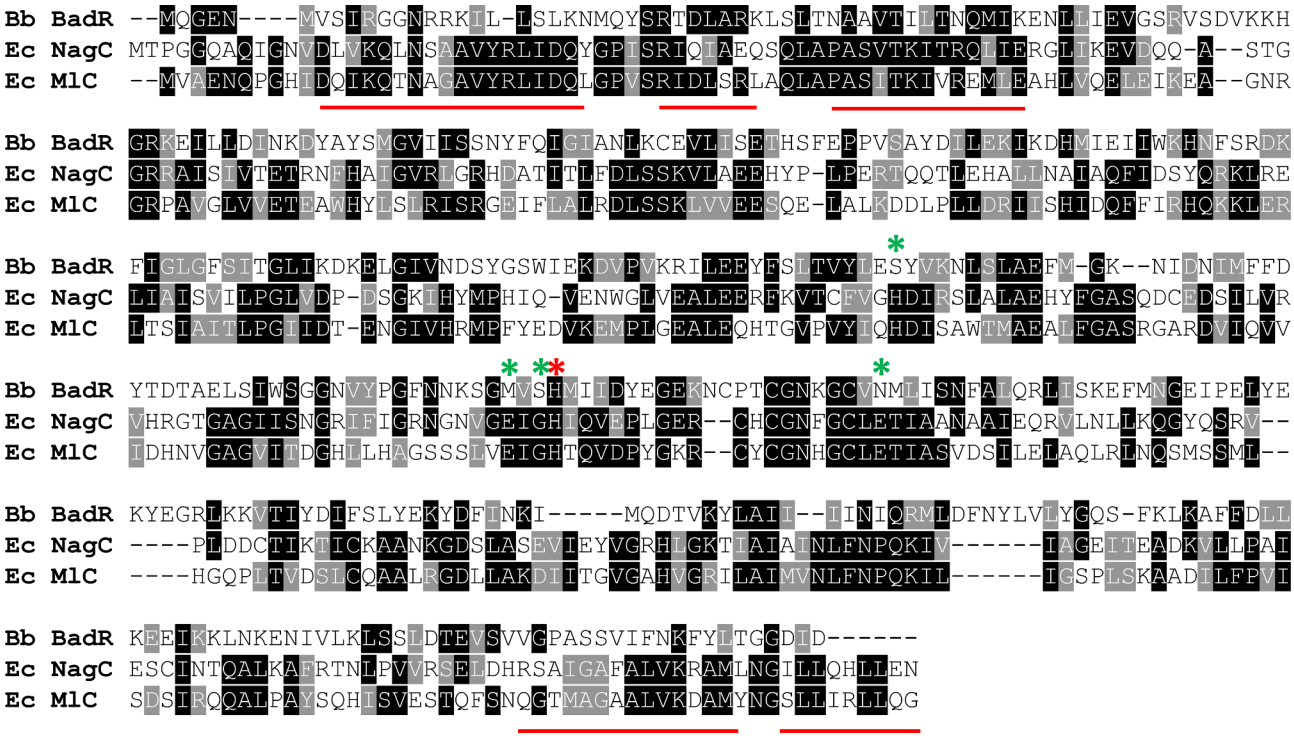

Fig. 7 Sequence alignment of BadR and its homologues. BadR was aligned with *E. coli* NagC and Mlc using the Clustal Omega Multiple Sequence Alignment Tool. Green star indicates amino acids involved in the binding of NagC to GlcNAc. Red star marks the residue required for the zinc binding of NagC and Mlc; this residue is conserved in BadR. Underlined regions outline the residues forming the N-terminal helix-turn-helix DNA binding domain and two C-terminal alpha-helices formed in NagC and Mlc

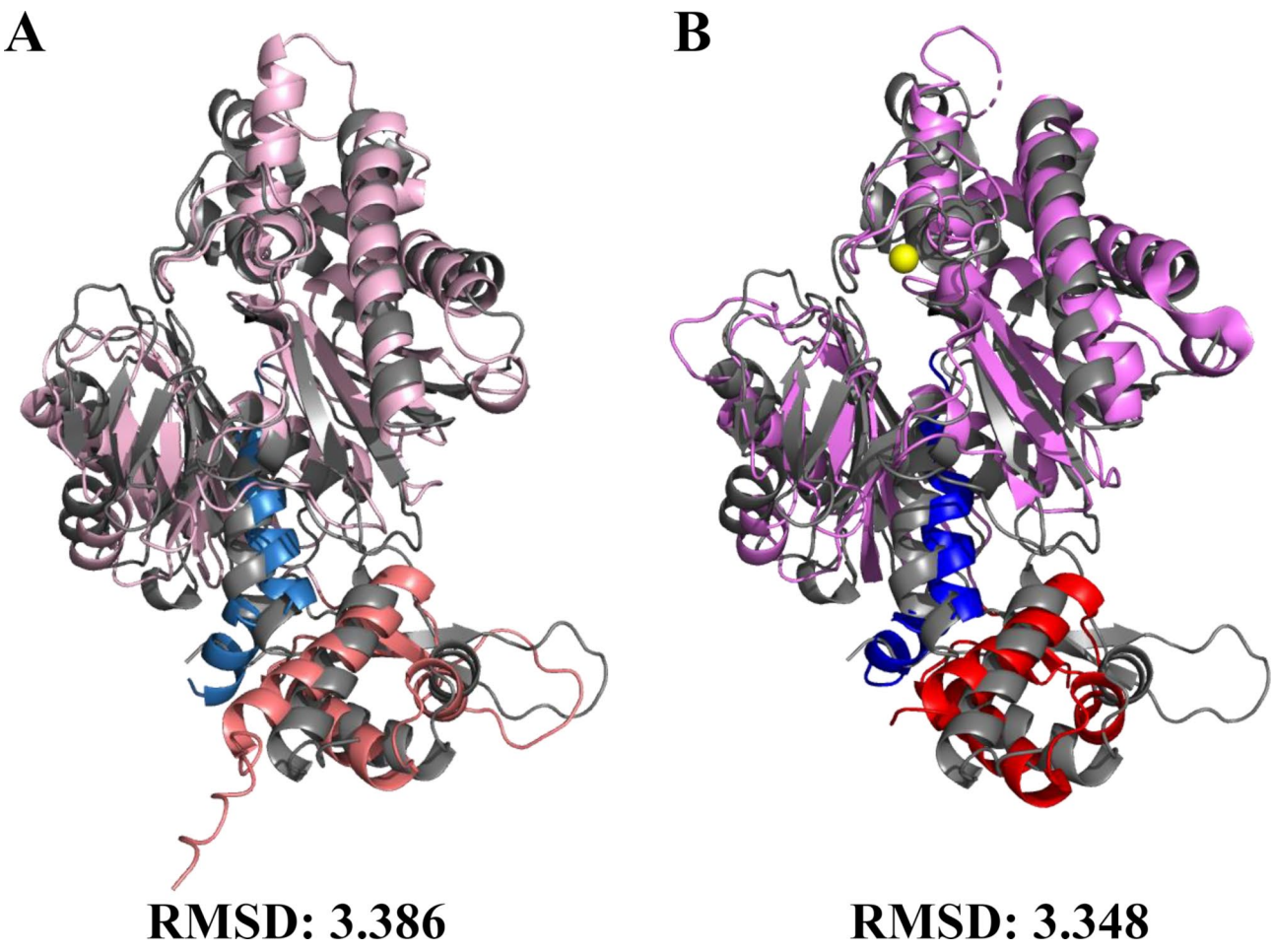

Fig. 8 Structure comparison of BadR and its homologues. The AlphaFold model structure of BadR was superimposed with the AlphaFold model structure of *E. coli* NagC **(A)** and the Mlc crystal structure (PDB: 1Z6R, Chain A) **(B)**. The structure of BadR is colored gray. In NagC and Mlc, the N-terminal DNA binding domains are colored in light and dark red; the C-terminal helices which loop to associate with the N-terminal DNA binding domain are colored in light and dark blue; and the C-terminal sugar binding domains conserved in ROK family proteins are colored in light and dark purple, respectively. A Zn molecule included with Mlc PDB structure is colored in yellow

In both NagC and Mlc, two C-terminal alpha helixes formed by residues 381–394 and 395–406 (Mlc numbering) loop towards the N-terminal DNA binding domain. However, analysis of hybrid NagC and Mlc proteins suggested that the association of these C-terminal helices with the HTH binding domain are only important for DNA-binding and inducer binding in Mlc [63]. Specifically, the C-terminal helices stabilize the interaction of Mlc with its inducer, glucose specific phosphotransferase (PtsG) protein $EIIB^{Glc}$ [64–66]. Mutation of the final C-terminal glycine (Gly406) renders Mlc incapable of binding to $EIIB^{Glc}$ [63]. Furthermore, removal of the Mlc C-terminal helices results in suboptimal DNA binding. No significant difference was observed in NagC DNA-binding or sugar binding when the corresponding residues were removed [63]. As shown in Fig. 7, BadR contains only three residues, Gly383, Lys393, and Gly399 found in the Mlc C-terminal helix 1 (Mlc residues 381–394) and lacks helix 2 (Mlc residues 395–406) altogether. Furthermore, BadR does not contain the final glycine residue (Mlc Gly406) essential for Mlc interaction with $EIIB^{Glc}$ and gene de-repression [63].

We also modeled the structure of BadR using AlphaFold and compared it with the structures of NagC and Mlc, respectively. Of note, the structure of Mlc was solved by X-ray crystallography (PDB: 1Z6R) [66], but the structure of NagC has not been experimentally determined. Therefore, we also modeled the structure of NagC using AlphaFold (Fig. S2). As shown in Fig. 8, the predicted BadR structure exhibited similarity to the NagC AlphaFold model (RMSD: 3.386) and the Mlc crystal structure (RMSD: 3.348). Interestingly, while our sequence analysis found that BadR lacks most residues forming the C-terminal helices important in Mlc, BadR is predicted to form a single C-terminal helix (residues 381–402) similar to Mlc C-terminal helix 1 that associates with the N-terminal DNA binding domain (Fig. 8B). Therefore, like Mlc, this C-terminal helix region may

also be important for the binding of BadR to DNA and/or inducer. Taken together, our in silico analyses suggest that BadR is structurally similar to NagC and Mlc, but the mechanism(s) by which BadR regulates gene expression may vary significantly from the regulatory mechanisms used by *E. coli* ROK family transcriptional regulators.

Discussion

The transcriptional regulator BadR is essential for *B. burgdorferi* infection in animals [17, 18]. To identify mammalian infection-associated genes regulated by BadR, Miller et al. cultivated WT *B. burgdorferi* and a *badR* mutant in BSK-II at 32 °C; spirochetes were collected at mid-logarithmic phase and gene expression was analyzed using microarray [17]. A total of 206 genes were differentially expressed in the *badR* mutant (≥ 2-fold change and $P \leq 0.05$), among which 127 genes were upregulated and 79 genes were downregulated. In another study, Arnold et al. cultivated WT *B. burgdorferi* and a *badR* mutant in BSK-II at 34 °C, collected spirochetes at mid-logarithmic phase, and analyzed gene expression using RNA-sequencing [20]. In total, 147 genes were found to be regulated by BadR; among these genes, 61 were upregulated and 86 were downregulated in the *badR* mutant. Interestingly, only 21 genes were identified in both studies. Herein, we also analyzed the BadR regulon in *B. burgdorferi* collected at the mid-logarithmic phase of growth. We optimized our in vitro cultivation conditions and grew spirochetes at 37 °C, the typical body temperature for mammals. Our results showed that 112 genes and 99 genes were upregulated or downregulated, respectively, in the *badR* mutant. Among these genes, 32 genes (~15%) were also found in the previous study by Arnold et al., whereas 71 genes (~34%) were identified in previous work by Miller et al. These discrepancies may result from the methods used for gene expression analysis (e.g., microarray vs. RNA-sequencing) and/or the culture conditions. Of note, the study by Arnold et al. [20] did not identify *rpoS* and RpoS-dependent *ospC* as differentially regulated by BadR. However, our study showed that expression of *rpoS*, *ospC*, and other RpoS-dependent genes were upregulated in the *badR* mutant, which is consistent with previous studies by Miller et al. and Ouyang et al. [17, 18]. Fifteen genes were identified in all three studies to be regulated by BadR; among these genes, *bbb04*, *bbb05*, and *bbb06* encoding chitobiose transporters were upregulated in the *badR* mutant. Moreover, 123 genes identified in this study were not reported in previous studies [17, 20]. These include 11 genes located on *lp54*, a plasmid important for tick transmission and mammalian infection, and 38 genes located on the highly conserved chromosome. Specifically, *lp6.6* (*bba66*) located on *lp54* was upregulated 5.2-fold in the *badR* mutant. This gene encodes a membrane associated protein important for transmission from ticks to mammals but is subsequently repressed in the mammalian host [67]. Therefore, BadR may repress *lp6.6* and other tick infection-associated genes when *B. burgdorferi* resides in the mammalian host. Genes downregulated in the *badR* mutant include chromosomal genes such as *bb0640*, *bb0641*, *bb0746*, and *bb0753*. These genes encode components of a spermidine specific ABC transporter (BB0640, BB0641) [68] and ABC transporter permeases (BB0754, BB0753) which may also be involved in the uptake of nutrients during mammalian infection.

Throughout the infectious lifecycle, *B. burgdorferi* are found in low numbers, except during tick feeding when nutrient-rich mammalian blood enters the tick midgut and triggers rapid bacterial replication [69]. During this time, cell density fluctuations in addition to other environmental factors, promote gene expression changes essential for bacterial tick-mammal transmission and mammalian infection. When *B. burgdorferi* is grown in BSK-II at 37 °C, cell density increases from the mid-logarithmic phase to stationary phase, partially mimicking this signal [9, 70, 71]. Consistent with the previous report [18], our data confirmed that the regulation of *rpoS* by BadR is growth-phase dependent. However, whether BadR regulates other genes in a growth phase-dependent manner remained unexplored. Therefore, we grew *B. burgdorferi* in BSK-II at 37 °C and collected spirochetes at the stationary phase for RNA-sequencing analysis. In total, 148 genes were upregulated in the mutant, among which 88 genes were upregulated at the stationary phase of growth only (but not at the mid-logarithmic phase). These included four genes located on *cp26*, a highly stable *B. burgdorferi* plasmid which carries the *resT* gene for DNA replication, *ospC* gene important for early mammalian infection, and possibly other genes important for cell survival and/or infectivity [72–74]. An additional 88 genes were downregulated at the stationary phase only, including 8 genes on *lp54*. Of these, *bba52*, encoding an outer membrane protein essential for transmission from the tick vector to mammalian host [75, 76], was downregulated 6.4-fold in the *badR* mutant. Furthermore, 37 genes located on the chromosome were downregulated including the *bb0665-bb0667* operon promoting cell division [77]. Interestingly, *bb0228* and *bb0794* were downregulated 3.2 and 2.8-fold in the *badR* mutant. *bb0228* encodes the BamB component of the BAM complex, whereas *bb0794* encodes a TamA homologue that directly interacts with the BAM complex (β-barrel assembly machine) in *B. burgdorferi* to properly assemble outer membrane proteins into the outer membrane [78–82]. Therefore, at high cell density, BadR may activate the expression of genes required for orienting lipoproteins in the outer membrane, a process essential for *B.*

burgdorferi survival and virulence. Taken together, these findings demonstrate that BadR regulates the expression of numerous genes in a growth phase-dependent manner.

Noteworthy, 60 and 38 genes were upregulated or downregulated, respectively, at both the mid-logarithmic phase and stationary phase of growth. A vast majority of these genes encode conserved hypothetical proteins or proteins of unknown function, making it difficult to discern the exact function of BadR at each growth phase. Moreover, numerous genes regulated by BadR at both growth phases are located on the *cp32* family plasmids and encode putative phage-virion assembly proteins, a finding consistent with the study by Miller et al. [17]. *B. burgdorferi* phage-virion assembly proteins have been speculated to be involved in horizontal gene transfer and enhancing genetic diversity during tick feeding, thus, providing a competitive advantage upon transmission to the mammalian host [83, 84]. Interestingly, *cp32* encoded prophages have also been shown to be regulated by the stringent response [85]. Additionally, at both the mid-logarithmic phase and stationary phase of growth, 98 BadR-regulated genes are located on infection-associated plasmids such as *lp25*, *lp54*, *lp28-4*, and *lp36*; 42 of these genes have unknown function and may encode novel virulence-associated proteins contributing to *B. burgdorferi* pathogenicity. The roles of these genes in *B. burgdorferi* infectivity will be investigated in future research.

In addition to a role for BadR during mammalian infection [17, 18], several lines of evidence support a role for this protein when *B. burgdorferi* resides in ticks. First, previous gene expression studies suggested that BadR regulates many genes located on plasmids associated with borrelial infection in ticks [17, 19, 20]. Second, BadR is expressed in *B. burgdorferi* not only under in vitro conditions mimicking unfed ticks, but also during the tick acquisition and intermolt phases [18]. Third, the *badR* mutant exhibits a growth defect when cultivated in vitro under conditions mimicking unfed ticks [17, 18]. Despite this, the transcriptional contribution of BadR during tick phases of the lifecycle has remained unexplored. Therefore, we performed RNA-sequencing of WT and the *badR* mutant grown under in vitro conditions mimicking unfed ticks. Our data showed that 79 genes were regulated by BadR under this condition. Specifically, 61 genes (77%) and 18 genes (23%) were upregulated or downregulated, respectively, in the *badR* mutant. Of those upregulated genes, 19 were located on *lp54*, a plasmid essential for tick transmission and host infection [3, 86, 87]. These included *bba65*, *bba66*, and *bba73* encoding immunogenic surface exposed lipoproteins; and *bba74* encoding a periplasmic protein important during tick feeding [88–91]. Furthermore, genes *bbk50*, *bbi39*, and *bbs41* were found to be upregulated in the *badR* mutant; these genes may contribute to the survival of *B. burgdorferi* in ticks and animal hosts [92–94]. Together, these data suggest that, when *B. burgdorferi* resides in the unfed tick, BadR represses genes required for tick-mammal transmission and/or mammalian infection. Noteworthy, when grown at 23 °C, at 37 °C to the mid-logarithmic phase, or at 37 °C to the stationary phase, 3, 25, and 14 chromosomal genes encoding housekeeping genes involved in basic biological processes such as metabolism, replication, transcription, and translation were downregulated in the *badR* mutant, respectively. Decreased expression of these genes is in good agreement with the impaired growth phenotype observed in *badR* deficient strains [17, 18].

To date, the mechanism by which BadR regulates gene expression remains unknown. Previous studies have shown that BadR binds directly to promoter DNA of *rpoS*, *bosR*, and *bb0240* [17–19]. However, the ability of phosphorylated sugars to bind BadR and cause its release from target DNA have been controversial. One study reported that BadR binding is alleviated by the addition of phosphorylated GlcNAC, glucose, xylulose, and ribose [17], whereas subsequent assays did not observe any change in BadR-DNA interaction when the same sugars were added [18, 19]. Like NagC and Mlc, the AlphaFold predicted structure of BadR contains an N-terminal DNA binding domain and a putative C-terminal sugar binding domain. However, BadR lacks many residues conserved in NagC and Mlc which facilitate binding to GlcNAC-6P or $EIIB^{Glc}$ [17, 63]. Moreover, BadR was found in this study to regulate expression of genes involved in the uptake and utilization of chitobiose, glycerol, and glucose. Thus, it appears unlikely that BadR functions like NagC and binds one specific phosphorylated sugar to alleviate protein-DNA interaction. If BadR is in fact a carbohydrate-responsive transcriptional regulator, this protein may instead have promiscuous binding activity for multiple carbohydrate substrates. Alternatively, if not a carbohydrate substrate, another growth-phase, or temperature dependent metabolite or co-factor may directly associate with BadR to alleviate DNA-binding. In this regard, the concentrations of multiple metabolites have been found to be increased when *B. burgdorferi* is grown in vitro [52, 95, 96]; one such metabolite may regulate the binding of BadR to target DNA. Additionally, as seen with Mlc, BadR may directly interact with a sugar transport protein(s) such as ChbC (BBB04), GlpF (BB0240), or another yet-to-be-identified protein, thereby sequestering BadR away from target DNA. These possibilities will be explored in the future.

Conclusions

In summary, by analyzing the BadR regulon in *B. burgdorferi* under various in vitro conditions, this work has provided several new insights regarding the contribution

of BadR to global gene regulation in *B. burgdorferi*. First, BadR regulates the expression of *rpoS* and RpoS-dependent genes in *B. burgdorferi*. Second, BadR is a global regulator and modulates the expression of different sets of genes under different conditions, suggesting a role for BadR during multiple phases of the tick-mammal infectious cycle. Although much remains to be studied about the underlying mechanism, BadR acts as a dual-function regulator to activate and repress gene expression. The BadR regulon likely are not only involved in basic cellular processes such as spirochete growth and replication, but also in borrelial parasitic strategies such as survival in unfed ticks as well as during tick feeding and mammalian infection. Additionally, this study has identified numerous novel BadR target genes, many of which encode proteins of unknown function. Further studies are warranted to investigate the physiological functions of these genes as well as their contributions to the infectious cycle of *B. burgdorferi*. Characterization of the BadR regulon will unveil novel virulence factors essential for *B. burgdorferi* adaptation and pathogenicity. It is worth noting that, although widely used in the research of *B. burgdorferi*, the in vitro culture conditions used in this study cannot fully mimic the tick or mammal conditions that *B. burgdorferi* encounters during its infectious cycle [58, 97]. Future work, such as defining the BadR regulon when *B. burgdorferi* resides in its natural tick and host environments, may provide more insight into the essential role of BadR during the tick-mammal infectious cycle of *B. burgdorferi*.

Supplementary Information

The online version contains supplementary material available at https://doi.org/10.1186/s12866-025-03797-9.

Supplementary Material 1

Supplementary Material 2

Acknowledgements
We thank Dr. Feng Cheng for his helpful discussion and guidance with RNA-sequencing data analysis and interpretation.

Author contributions
SG and ZO designed the study, performed the experiments, analyzed, and interpreted the results, and wrote the manuscript. All authors read and approved the manuscript.

Funding
This work was supported by funding from the National Institutes of Health AI146909, AI159061, and AI152983. The funders had no role in the conceptualization, design, data collection, analysis, decision to publish, or preparation of this manuscript.

Data availability
The datasets generated and analyzed during the current study are available in the GEO repository with accession number GSE277958, https://www.ncbi.nlm.nih.gov/geo/query/acc.cgi? acc=GSE277958.

Declarations

Ethics approval and consent to participate
Not applicable.

Consent for publication
Not applicable.

Competing interests
The authors declare no competing interests.

Received: 22 October 2024 / Accepted: 29 January 2025
Published online: 26 February 2025

References

1. Helble JD, McCarthy JE, Hu LT. Interactions between *Borrelia burgdorferi* and its hosts across the enzootic cycle. Parasite Immunol. 2021;43(5):e12816.
2. Radolf JD, Caimano MJ, Stevenson B, Hu LT. Of ticks, mice and men: understanding the dual-host lifestyle of Lyme disease spirochaetes. Nat Rev Microbiol. 2012;10(2):87–99.
3. Caimano MJ, Drecktrah D, Kung F, Samuels DS. Interaction of the Lyme disease spirochete with its tick vector. Cell Microbiol. 2016;18(7):919–27.
4. Ojaimi C, Brooks C, Casjens S, Rosa P, Elias A, Barbour A, et al. Profiling of temperature-induced changes in *Borrelia burgdorferi* gene expression by using whole genome arrays. Infect Immun. 2003;71(4):1689–705.
5. Ramamoorthy R, Scholl-Meeker D. *Borrelia burgdorferi* proteins whose expression is similarly affected by culture temperature and pH. Infect Immun. 2001;69(4):2739–42.
6. Corona A, Schwartz I. *Borrelia burgdorferi*: carbon metabolism and the tick-mammal enzootic cycle. Microbiol Spectr. 2015;3(3). https://doi.org/10.1128/microbiolspec.mbp-0011-2014.
7. Bontemps-Gallo S, Lawrence K, Gherardini FC. Two different virulence-related regulatory pathways in *Borrelia burgdorferi* are directly affected by osmotic fluxes in the blood meal of feeding *Ixodes ticks*. PLoS Pathog. 2016;12(8):e1005791.
8. Schwan TG, Piesman J, Golde WT, Dolan MC, Rosa PA. Induction of an outer surface protein on Borrelia burgdorferi during tick feeding. Proc Natl Acad Sci. 1995;92(7):2909–13.
9. Yang X, Goldberg MS, Popova TG, Schoeler GB, Wikel SK, Hagman KE, et al. Interdependence of environmental factors influencing reciprocal patterns of gene expression in virulent *Borrelia burgdorferi*. Mol Microbiol. 2000;37(6):1470–9.
10. Samuels DS, Lybecker MC, Yang XF, Ouyang Z, Bourret TJ, Boyle WK, et al. Gene regulation and transcriptomics. Curr Issues Mol Biol. 2021;42(1):223–66.
11. Caimano MJ, Groshong AM, Belperron A, Mao J, Hawley KL, Luthra A, et al. The RpoS gatekeeper in *Borrelia burgdorferi*: an Invariant Regulatory Scheme that promotes spirochete persistence in Reservoir hosts and Niche Diversity. Front Microbiol. 2019;10:1923.
12. Fisher MA, Grimm D, Henion AK, Elias AF, Stewart PE, Rosa PA et al. *Borrelia burgdorferi* σ^{54} is required for mammalian infection and vector transmission but not for tick colonization. Proceedings of the National Academy of Sciences. 2005;102(14):5162-7.
13. Hübner A, Yang X, Nolen DM, Popova TG, Cabello FC, Norgard MV. Expression of *Borrelia burgdorferi* OspC and DbpA is controlled by a RpoN-RpoS regulatory pathway. Proc Natl Acad Sci U S A. 2001;98(22):12724–9.
14. Ouyang Z, Blevins JS, Norgard MV. Transcriptional interplay among the regulators Rrp2, RpoN and RpoS in *Borrelia burgdorferi*. Microbiology. 2008;154(9):2641–58.
15. Caimano MJ, Iyer R, Eggers CH, Gonzalez C, Morton EA, Gilbert MA, et al. Analysis of the RpoS regulon in *Borrelia burgdorferi* in response to mammalian host signals provides insight into RpoS function during the enzootic cycle. Mol Microbiol. 2007;65(5):1193–217.
16. Ouyang Z, Narasimhan S, Neelakanta G, Kumar M, Pal U, Fikrig E, et al. Activation of the RpoN-RpoS regulatory pathway during the enzootic life cycle of *Borrelia burgdorferi*. BMC Microbiol. 2012;12:1–9.
17. Miller CL, Karna SR, Seshu J. Borrelia host adaptation Regulator (BadR) regulates *rpoS* to modulate host adaptation and virulence factors in *Borrelia burgdorferi*. Mol Microbiol. 2013;88(1):105–24.

18. Ouyang Z, Zhou J. BadR (BB0693) controls growth phase-dependent induction of *rpoS* and *bosR* in *Borrelia burgdorferi* via recognizing TAAAATAT motifs. Mol Microbiol. 2015;98(6):1147–67.
19. Zhang J-J, Raghunandanan S, Wang Q, Priya R, Alanazi F, Lou Y, et al. BadR directly represses the expression of the glycerol utilization operon in the Lyme disease pathogen. J Bacteriol. 2024;206(2):e00340–23.
20. Arnold WK, Savage CR, Lethbridge KG, Smith TC 2, Brissette CA, Seshu J, et al. Transcriptomic insights on the virulence-controlling CsrA, BadR, RpoN, and RpoS regulatory networks in the Lyme disease spirochete. PLoS ONE. 2018;13(8):e0203286.
21. Ouyang Z, Deka RK, Norgard MV. BosR (BB0647) controls the RpoN-RpoS regulatory pathway and virulence expression in *Borrelia burgdorferi* by a novel DNA-binding mechanism. PLoS Pathog. 2011;7(2):e1001272.
22. Boylan JA, Posey JE, Gherardini FC. *Borrelia* oxidative stress response regulator, BosR: a distinctive Zn-dependent transcriptional activator. Proceedings of the National Academy of Sciences. 2003;100(20):11684-9.
23. Hyde JA, Shaw DK, Smith R III, Trzeciakowski JP, Skare JT. The BosR regulatory protein of *Borrelia burgdorferi* interfaces with the RpoS regulatory pathway and modulates both the oxidative stress response and pathogenic properties of the Lyme disease spirochete. Mol Microbiol. 2009;74(6):1344–55.
24. Ouyang Z, Kumar M, Kariu T, Haq S, Goldberg M, Pal U, et al. BosR (BB0647) governs virulence expression in *Borrelia burgdorferi*. Mol Microbiol. 2009;74(6):1331–43.
25. Yang XF, Alani SM, Norgard MV. The response regulator Rrp2 is essential for the expression of major membrane lipoproteins in *Borrelia burgdorferi*. Proceedings of the National Academy of Sciences. 2003;100(19):11001-6.
26. Ouyang Z, Zhou J, Norgard MV. Synthesis of RpoS is dependent on a putative enhancer binding protein Rrp2 in *Borrelia burgdorferi*. PLoS ONE. 2014;9(5):e96917.
27. Groshong AM, Gibbons NE, Yang XF, Blevins JS. Rrp2, a prokaryotic enhancer-like binding protein, is essential for viability of *Borrelia burgdorferi*. J Bacteriol. 2012;194(13):3336–42.
28. Jusufovic N, Krusenstjerna AC, Savage CR, Saylor TC, Brissette CA, Zückert WR et al. *Borrelia burgdorferi* PlzA is a cyclic-di-GMP dependent DNA and RNA binding protein. Mol Microbiol. 2024.
29. Grassmann AA, Tokarz R, Golino C, McLain MA, Groshong AM, Radolf JD et al. BosR and PlzA reciprocally regulate RpoS function to sustain *Borrelia burgdorferi* in ticks and mammals. J Clin Investig. 2023;133(5).
30. Pitzer JE, Sultan SZ, Hayakawa Y, Hobbs G, Miller MR, Motaleb MA. Analysis of the *Borrelia burgdorferi* cyclic-di-GMP-binding protein PlzA reveals a role in motility and virulence. Infect Immun. 2011;79(5):1815–25.
31. Freedman JC, Rogers EA, Kostick JL, Zhang H, Iyer R, Schwartz I, et al. Identification and molecular characterization of a cyclic-di-GMP effector protein, PlzA (BB0733): additional evidence for the existence of a functional cyclic-di-GMP regulatory network in the Lyme disease spirochete, Borrelia burgdorferi. FEMS Immunol Med Microbiol. 2010;58(2):285–94.
32. He M, Zhang J-J, Ye M, Lou Y, Yang XF. Cyclic di-GMP receptor PlzA controls virulence gene expression through RpoS in *Borrelia burgdorferi*. Infect Immun. 2014;82(1):445–52.
33. Van Gundy T, Patel D, Bowler BE, Rothfuss MT, Hall AJ, Davies C, et al. c-di-GMP regulates activity of the PlzA RNA chaperone from the Lyme disease spirochete. Mol Microbiol. 2023;119(6):711–27.
34. Karna SR, Sanjuan E, Esteve-Gassent MD, Miller CL, Maruskova M, Seshu J. CsrA modulates levels of lipoproteins and key regulators of gene expression critical for pathogenic mechanisms of *Borrelia burgdorferi*. Infect Immun. 2011;79(2):732–44.
35. Sze CW, Li C. Inactivation of *bb0184*, which encodes carbon storage regulator A, represses the infectivity of *Borrelia burgdorferi*. Infect Immun. 2011;79(3):1270–9.
36. Ouyang Z, Zhou J, Norgard MV. CsrA (BB0184) is not involved in activation of the RpoN-RpoS regulatory pathway in *Borrelia burgdorferi*. Infect Immun. 2014;82(4):1511–22.
37. Savage CR, Jutras BL, Bestor A, Tilly K, Rosa PA, Tourand Y, et al. *Borrelia burgdorferi* SpoVG DNA-and RNA-binding protein modulates the physiology of the Lyme disease spirochete. J Bacteriol. 2018;200(12). 10.1128/jb. 00033– 18.
38. Saylor TC, Savage CR, Krusenstjerna AC, Jusufovic N, Zückert WR, Brissette CA et al. Quantitative analyses of interactions between SpoVG and RNA/DNA. Biochemical and biophysical research communications. 2023;654:40–6.
39. Thompson C, Mason C, Parrilla S, Ouyang Z. The Lon-1 protease is required by *Borrelia burgdorferi* to infect the mammalian host. Infect Immun. 2020;88(6):e00951–19.
40. Mason C, Thompson C, Ouyang Z. The Lon-2 protease of *Borrelia burgdorferi* is critical for infection in the mammalian host. Mol Microbiol. 2020;113(5):938–50.
41. Mason C, Thompson C, Ouyang Z. DksA plays an essential role in regulating the virulence of *Borrelia burgdorferi*. Mol Microbiol. 2020;114(1):172–83.
42. Thompson C, Waldron C, George S, Ouyang Z. Role of the hypothetical protein BB0563 during *Borrelia burgdorferi* infection in animals. Infect Immun. 2023;91(3):e00539–22.
43. Livak KJ, Schmittgen TD. Analysis of relative gene expression data using real-time quantitative PCR and the $2^{(-\text{Delta Delta C(T)})}$ method. Methods. 2001;25(4):402–8.
44. Pfaffl MW. Quantification strategies in real-time PCR. AZ Quant PCR. 2004;1:89–113.
45. Wang J, Chitsaz F, Derbyshire MK, Gonzales NR, Gwadz M, Lu S, et al. The conserved domain database in 2023. Nucleic Acids Res. 2023;51(D1):D384–8.
46. Altschul SF, Gish W, Miller W, Myers EW, Lipman DJ. Basic local alignment search tool. J Mol Biol. 1990;215(3):403–10.
47. Smith AH, Blevins JS, Bachlani GN, Yang XF, Norgard MV. Evidence that RpoS (σ^S) in *Borrelia burgdorferi* is controlled directly by RpoN (σ^{54}/σ^N). J Bacteriol. 2007;189(5):2139–44.
48. Groshong AM, Grassmann AA, Luthra A, McLain MA, Provatas AA, Radolf JD, et al. PlzA is a bifunctional c-di-GMP biosensor that promotes tick and mammalian host-adaptation of *Borrelia burgdorferi*. PLoS Pathog. 2021;17(7):e1009725.
49. Stevenson B. The Lyme disease spirochete, *Borrelia burgdorferi*, as a model vector-borne pathogen: insights on regulation of gene and protein expression. Curr Opin Microbiol. 2023;74:102332.
50. Pappas CJ, Iyer R, Petzke MM, Caimano MJ, Radolf JD, Schwartz I. *Borrelia burgdorferi* requires glycerol for maximum fitness during the tick phase of the enzootic cycle. PLoS Pathog. 2011;7(7):e1002102.
51. He M, Ouyang Z, Troxell B, Xu H, Moh A, Piesman J, et al. Cyclic di-GMP is essential for the survival of the Lyme disease spirochete in ticks. PLoS Pathog. 2011;7(6):e1002133.
52. Drecktrah D, Hall LS, Crouse B, Schwarz B, Richards C, Bohrnsen E, et al. The glycerol-3-phosphate dehydrogenases GpsA and GlpD constitute the oxidoreductive metabolic linchpin for Lyme disease spirochete host infectivity and persistence in the tick. PLoS Pathog. 2022;18(3):e1010385.
53. von Lackum K, Stevenson B. Carbohydrate utilization by the Lyme borreliosis spirochete, *Borrelia burgdorferi*. FEMS Microbiol Lett. 2005;243(1):173–9.
54. Lybecker MC, Samuels DS. Temperature-induced regulation of RpoS by a small RNA in *Borrelia burgdorferi*. Mol Microbiol. 2007;64(4):1075–89.
55. Fraser CM, Casjens S, Huang WM, Sutton GG, Clayton R, Lathigra R, et al. Genomic sequence of a Lyme disease spirochaete, *Borrelia burgdorferi*. Nature. 1997;390(6660):580–6.
56. Titgemeyer F, Reizer J, Reizer A, Saier MH Jr. Evolutionary relationships between sugar kinases and transcriptional repressors in bacteria. Microbiology. 1994;140(9):2349–54.
57. Kazanov MD, Li X, Gelfand MS, Osterman AL, Rodionov DA. Functional diversification of ROK-family transcriptional regulators of sugar catabolism in the *Thermotogae* phylum. Nucleic Acids Res. 2013;41(2):790–803.
58. Iyer R, Caimano MJ, Luthra A, Axline D Jr, Corona A, Iacobas DA, et al. Stage-specific global alterations in the transcriptomes of L yme disease spirochetes during tick feeding and following mammalian host adaptation. Mol Microbiol. 2015;95(3):509–38.
59. Casjens S, Palmer N, Van Vugt R, Mun Huang W, Stevenson B, Rosa P, et al. A bacterial genome in flux: the twelve linear and nine circular extrachromosomal DNAs in an infectious isolate of the Lyme disease spirochete *Borrelia burgdorferi*. Mol Microbiol. 2000;35(3):490–516.
60. Casjens SR, Mongodin EF, Qiu WG, Luft BJ, Schutzer SE, Gilcrease EB, et al. Genome stability of Lyme disease spirochetes: comparative genomics of *Borrelia burgdorferi* plasmids. PLoS ONE. 2012;7(3):e33280.
61. Rhodes RG, Atoyan JA, Nelson DR. The chitobiose transporter, *chbC*, is required for chitin utilization in *Borrelia burgdorferi*. BMC Microbiol. 2010;10:1–14.
62. Richards CL, Raffel SJ, Bontemps-Gallo S, Dulebohn DP, Herbert TC, Gherardini FC. The arginine deaminase system plays distinct roles in *Borrelia burgdorferi* and *Borrelia hermsii*. PLoS Pathog. 2022;18(3):e1010370.
63. Pennetier C, Domínguez-Ramírez L, Plumbridge J. Different regions of Mlc and NagC, homologous transcriptional repressors controlling expression of the glucose and N-acetylglucosamine phosphotransferase systems in *Escherichia coli*, are required for inducer signal recognition. Mol Microbiol. 2008;67(2):364–77.

64. Nam TW, Cho SH, Shin D, Kim JH, Jeong JY, Lee JH et al. The *Escherichia coli* glucose transporter enzyme IICB^{Glc} recruits the global repressor Mlc. EMBO J. 2001.
65. Seitz S, Lee S-J, Pennetier C, Boos W, Plumbridge J. Analysis of the interaction between the global regulator Mlc and EIIB^{Glc} of the glucose-specific phosphotransferase system in *Escherichia coli*. J Biol Chem. 2003;278(12):10744–51.
66. Schiefner A, Gerber K, Seitz S, Welte W, Diederichs K, Boos W. The crystal structure of Mlc, a global regulator of sugar metabolism in *Escherichia coli*. J Biol Chem. 2005;280(32):29073–9.
67. Promnares K, Kumar M, Shroder DY, Zhang X, Anderson JF, Pal U. *Borrelia burgdorferi* small lipoprotein *Lp*6. 6 is a member of multiple protein complexes in the outer membrane and facilitates pathogen transmission from ticks to mice. Mol Microbiol. 2009;74(1):112–25.
68. Bontemps-Gallo S, Lawrence KA, Richards CL, Gherardini FC. *Borrelia burgdorferi* genes, *bb0639-0642*, encode a putative putrescine/spermidine transport system, PotABCD, that is spermidine specific and essential for cell survival. Mol Microbiol. 2018;108(4):350–60.
69. Piesman J, Oliver JR, Sinsky RJ. Growth kinetics of the Lyme disease spirochete (*Borrelia burgdorferi*) in vector ticks (*Ixodes dammini*). Am J Trop Med Hyg. 1990;42(4):352–7.
70. Ramamoorthy R, Philipp MT. Differential expression of *Borrelia burgdorferi* proteins during growth *in vitro*. Infect Immun. 1998;66(11):5119–24.
71. Jutras BL, Chenail AM, Stevenson B. Changes in bacterial growth rate govern expression of the *Borrelia burgdorferi* OspC and Erp infection-associated surface proteins. J Bacteriol. 2013;195(4):757–64.
72. Byram R, Stewart PE, Rosa P. The essential nature of the ubiquitous 26-kilobase circular replicon of *Borrelia burgdorferi*. J Bacteriol. 2004;186(11):3561–9.
73. Tilly K, Casjens S, Stevenson B, Bono JL, Samuels DS, Hogan D, et al. The *Borrelia burgdorferi* circular plasmid *cp26*: conservation of plasmid structure and targeted inactivation of the *ospC* gene. Mol Microbiol. 1997;25(2):361–73.
74. Tilly K, Checroun C, Rosa PA. Requirements for *Borrelia burgdorferi* plasmid maintenance. Plasmid. 2012;68(1):1–12.
75. Kumar M, Yang X, Coleman AS, Pal U. BBA52 facilitates *Borrelia burgdorferi* transmission from feeding ticks to murine hosts. J Infect Dis. 2010;201(7):1084–95.
76. Kumar M, Kaur S, Kariu T, Yang X, Bossis I, Anderson JF, et al. *Borrelia burgdorferi* BBA52 is a potential target for transmission blocking Lyme disease vaccine. Vaccine. 2011;29(48):9012–9.
77. Yang Y, Li C. Transcription and genetic analyses of a putative N-acetylmuramyl-L-alanine amidase in *Borrelia burgdorferi*. FEMS Microbiol Lett. 2009;290(2):164–73.
78. Iqbal H, Kenedy MR, Lybecker M, Akins DR. The TamB ortholog of *Borrelia burgdorferi* interacts with the β-barrel assembly machine (BAM) complex protein BamA. Mol Microbiol. 2016;102(5):757–74.
79. Lenhart TR, Akins DR. *Borrelia burgdorferi* locus BB0795 encodes a BamA orthologue required for growth and efficient localization of outer membrane proteins. Mol Microbiol. 2010;75(3):692–709.
80. Lenhart TR, Kenedy MR, Yang X, Pal U, Akins DR. BB0324 and BB0028 are constituents of the *Borrelia burgdorferi* β-barrel assembly machine (BAM) complex. BMC Microbiol. 2012;12:1–12.
81. Dunn JP, Kenedy MR, Iqbal H, Akins DR. Characterization of the β-barrel assembly machine accessory lipoproteins from *Borrelia burgdorferi*. BMC Microbiol. 2015;15:1–16.
82. Hall KT, Kenedy MR, Johnson DK, Hefty PS, Akins DR. A conserved C-terminal domain of TamB interacts with multiple BamA POTRA domains in *Borreliella burgdorferi*. PLoS ONE. 2024;19(8):e0304839.
83. Faith DR, Kinnersley M, Brooks DM, Drecktrah D, Hall LS, Luo E, et al. Characterization and genomic analysis of the Lyme disease spirochete bacteriophage ϕBB-1. PLoS Pathog. 2024;20(4):e1012122.
84. Eggers CH, Kimmel BJ, Bono JL, Elias AF, Rosa P, Samuels DS. Transduction by φBB-1, a bacteriophage of *Borrelia burgdorferi*. J Bacteriol. 2001;183(16):4771–8.
85. Drecktrah D, Lybecker M, Popitsch N, Rescheneder P, Hall LS, Samuels DS. The *Borrelia burgdorferi* RelA/SpoT homolog and stringent response regulate survival in the tick vector and global gene expression during starvation. PLoS Pathog. 2015;11(9):e1005160.
86. Stewart PE, Byram R, Grimm D, Tilly K, Rosa PA. The plasmids of *Borrelia burgdorferi*: essential genetic elements of a pathogen. Plasmid. 2005;53(1):1–13.
87. Pal U, Kitsou C, Drecktrah D, Yas OB, Fikrig E. Interactions between ticks and lyme disease spirochetes. Curr Issues Mol Biol. 2021;42(1):113–44.
88. Clifton DR, Nolder CL, Hughes JL, Nowalk AJ, Carroll JA. Regulation and expression of *bba66* encoding an immunogenic infection-associated lipoprotein in *Borrelia burgdorferi*. Mol Microbiol. 2006;61(1):243–58.
89. Hughes JL, Nolder CL, Nowalk AJ, Clifton DR, Howison RR, Schmit VL, et al. *Borrelia burgdorferi* surface-localized proteins expressed during persistent murine infection are conserved among diverse *Borrelia spp*. Infect Immun. 2008;76(6):2498–511.
90. Mulay VB, Caimano MJ, Iyer R, Dunham-Ems S, Liveris D, Petzke MM, et al. *Borrelia burgdorferi bba74* is expressed exclusively during tick feeding and is regulated by both arthropod-and mammalian host-specific signals. J Bacteriol. 2009;191(8):2783–94.
91. Mulay V, Caimano MJ, Liveris D, Desrosiers DC, Radolf JD, Schwartz I. *Borrelia burgdorferi* BBA74, a periplasmic protein associated with the outer membrane, lacks porin-like properties. J Bacteriol. 2007;189(5):2063–8.
92. Fikrig E, Feng W, Barthold SW, Telford SR, Flavell RA. Arthropod-and host-specific *Borrelia burgdorferi bbk32* expression and the inhibition of spirochete transmission. J Immunol. 2000;164(10):5344–51.
93. Singh P, Verma D, Backstedt BT, Kaur S, Kumar M, Smith AA, et al. *Borrelia burgdorferi* BBI39 paralogs, targets of protective immunity, reduce pathogen persistence either in hosts or in the vector. J Infect Dis. 2017;215(6):1000–9.
94. Xu Y, Bruno JF, Luft BJ. Profiling the humoral immune response to *Borrelia burgdorferi* infection with protein microarrays. Microb Pathog. 2008;45(5–6):403–7.
95. Glader O, Puljula E, Jokioja J, Karonen M, Sinkkonen J, Hytönen J. NMR metabolome of *Borrelia burgdorferi in vitro* and *in vivo* in mice. Sci Rep. 2019;9(1):8049.
96. Ramos D, Lasseter AG, Richards CL, Schwarz B, Ghosh S, Victoria B, et al. Riboflavin salvage by *Borrelia burgdorferi* supports carbon metabolism and is essential for survival in the tick vector. Mol Microbiol. 2022;118(4):443–56.
97. Sapiro AL, Hayes BM, Volk RF, Zhang JY, Brooks DM, Zhao Z, Kinnersley M, Secor PR. Longitudinal map of transcriptome changes in the Lyme pathogen. *Borrelia burgdorferi* during tick-borne transmission. Elife. 2023;(1)12:RP86636.

Publisher's note